RESEARCH PAPER

Fabrication and Simulation Properties of [SiO_2 - TiO_2] / Silan-Cellulose Acetate Nanocomposite for Self-Clean Surfaces Applications

Ali N. Saleh [1], Bahjat B. Kadhim [1], Husham M. Fadhel [2]*

[1] *Department of Physics, College of Science, Mustansiriyah University, Baghdad, Iraq*

[2] *Ministry of Science and Technology, Baghdad, Iraq*

ARTICLE INFO

Article History:
Received 12 April 2022
Accepted 27 June 2022
Published 01 July 2022

Keywords:
Contact angle
Nanocomposite
Super hydrophobic
Self-clean surface
Thermal spray coating

ABSTRACT

In this work, nanocomposite films (SiO_2-TiO_2 / silan-cellulose acetate) fabricated by thermal spray coating method on heated glass substrates at 70 Celsius Degree. The adding (0, 10:1, 10:2, 10:3, 10:4) of (SiO_2:TiO_2) weight ratio was increased the water contact angle. The films have a good adhesion with glass substrates. All specimens have hydrophobic property. The process of preparing the hydrophobic composites was simulated, in addition to the simulation of the structural properties. The simulation was carried out using Gaussian program by employing Gauss view studio using density functional theory. The experimental results were compared with the simulation results, and they were of excellent agreement. The simulation results helped in analyzing and interpreting the practical results in a comprehensive manner. It can be concluded that the contact angles that content TiO_2 nanoparticles of the films were greater than that of the pure film. The optimal value of weight ratio was at the ratio 10: 3 with a contact angle equal to 156.2, so the films acquired the super hydrophobic surfaces. Moreover, it can be concluded that the simulation was able to analyze the surface property of the composite and the reason for it having a hydrophobic property.

How to cite this article
Saleh A N., Kadhim B B., Fadhel H M.. Fabrication and Simulation Properties of [SiO_2 - TiO_2] / Silan-Cellulose Acetate Nanocomposite for Self-Clean Surfaces Applications. J Nanostruct, 2022; 12(3):580-587. DOI: 10.22052/JNS.2022.03.011

INTRODUCTION

The non-wettability was observed in Nature such as in cicada's wings and the lotus leaves [1, 2]. Lotus leaves showed fantastic properties of Wetness and self-cleaning surface "hydrophobicity", typically determined by measuring the contact angle between the surface and the drop of water [3]. The super hydrophobic feature of any surface is defined as a situation where the drop of water is similar to the spherical shape, causing the drop of water to slide and roll on the surface even when the angle of deviation of the surface from the horizon "droplet angle" is very small. That is, when the contact angle is greater than 150 degrees and the droplet angle less than 10 degrees, superhydrophobic surfaces have numerous applications in industries. Super hydrophobicity can be obtained by controlling the roughness of the surface and the surface energy [4].

The surface acquires the status of hydrophobic when the topography of the surface contains nano and microstructure named hierarchical structure using materials having a low surface free energy.

* *Corresponding Author Email: sci.phy.bbk@uomustansiriyah.edu.iq*

Self-clean surfaces

can be manufactured in many physical and chemical preparation methods [2, 5]. Certain chemical compounds such as silan can be used to manufacture self-clean surfaces because they have low surface energy and can coat on different types of substrates [6].

Thermal spray coating has a great interest when preparing self-clean films for its advantage of low cost, ease of work and the possibility of mixing several materials with each other, and substrate independence [7–8]. Li researcher developed coatings that have super hydrophobic coatings property using spraying technique lay-by-lay added materials [9]. Using the one-step method, Li et al. researchers enabled to manufacture of colorful superhydrophobic surfaces by spraying inorganic materials on metal substrates [10]. Wang et al. used micro and particles in addition to the polymer to obtain compositions with low surface energy to fabricate super hydrophobic surfaces deposited on the substrates of the magnesium alloy [11]. Hydrophobic coatings are adopted by spray technique is mostly used for the aggregation of hydrophobic and low surface energy particles [12]. Silicon dioxide is widely used to manufacture superhydrophobic surfaces [13, 14] because it's low cost, low toxicity, environmentally friendly and chemically stable. One-step thermal spraying technique has been used to manufacture polymer nanocomposite film One-step thermal spraying technique used to manufacture polymer nanocomposite film (polydimethyldiclorosilane/ SiO_2- TiO_2) which characterized by high adhesion and through which large areas and various surfaces of materials can be painted.

As it is known and scientifically proven, simulation is used for the purpose of obtaining results that increase the accuracy of the practical results, in addition to knowing the comparison between them to reach congruence.

Recently, the Gaussian program has been used to implement simulations, especially in the field of materials science, where the Gaussian program depends on calculating the total energy of the system by applying the Schrödinger equation to the particles of the system using one of the theories of quantum mechanics according to a basis set and functions that describe the system. Gaussian program can perform simulations to prepare the molecules under study to calculate the structural, vibrational, optical, thermal and mechanical properties [15 – 17].

THEORETICAL CONSIDERATIONS

The contact angle can be defined as the angle formed between the surface and the tangent is drawn on the edge of the drop of water at the seam point between the surface and the drop (Fig. 1a). Based on the roughness and homogeneity of the topography of the surface, there are two models (Wenzel CA and Cassie CA) for interpreting the hydrophobic and hydrophilic phenomenon. When the water drop balanced on any homogeneous solid chemical surface, the contact angle called Young's contact angle, as can be seen from the Fig. 1a.

Practically it is difficult to get a homogeneous surface ideal for sliding the drop of water because there must be a variation in the roughness and topography of the surface. The decrease on these surfaces can be in the case of stable balance, or the case of unstable balance, specifically the phenomenon of contact angle hysteria. Due

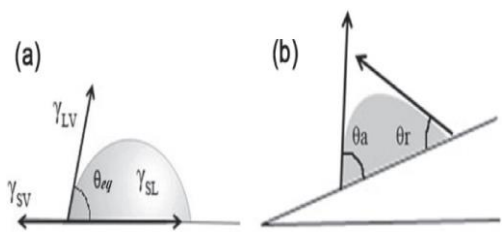

Fig. 1. Schematic illustration of (a) contact angle ª on the flat solid surface and (b) a stable droplet on the tilted surface owing to the contact angle hysteresis, advancing angle ªa and receding angle [18].

to contact angle hysteria, when the surface is assigned at a certain angle and the drop can be stable in the form of a slope (1b), the contact angle becomes larger or smaller, i.e. the angle of progress or the shape of the receding angle (1b). If not for the contact angle, the drop of water will roll from the surface [18].

Fig. 1: Schematic illustration of (a) contact angle ª on the flat solid surface and (b) a stable droplet on the tilted surface owing to the contact angle hysteresis, advancing angle ªa and receding angle [18].

One of the theories of quantum mechanics is used in simulations implemented through the Gaussian program. One of the most significant methods to calculate the electronic structure of solids, molecules and atoms is Density functional theory (DFT). Having been on a large scale used for over 40 years by physicists working on the electronic properties of surfaces, defects solids, etc., DFT based on the distribution of electron density n(r), instead of many-electron wave function Ψ (r_1, r_2, r_3...) [19].

The central quantity in DFT is the electron density ρ(r). It is defined as the integral over the spin coordinates of all electrons and over all but one of the spatial variables (x=r,s):

$$\rho(r) = N \int \dots\dots\dots \int |\Psi(\vec{x}_1, \vec{x}_2, \dots \vec{x}_N)| \, ds_1 \, d\vec{x}_2 \dots\dots \, d\vec{x}_N \quad (1)$$

Where ρ(r) represent probability of existence any electrons inside a volume element dr. Because ρ(r) represents the probability, this means that ρ(r) is a nonnegative function and vanishes at infinity and integrates to the total number of electrons N i.e [87] 23:

$$\rho(\vec{r} \to \infty) = 0$$
$$\int \rho(\vec{r}) d(\vec{r}) = N \quad (2)$$

Density functional theory is very successful approach for the description of ground state properties of metals, semiconductors, and insulators. The success of density functional theory (DFT) not only involve standard bulk materials but also complex materials such as proteins and carbon nanotubes, While DFT in principle gives a good depiction of ground case characteristic, practical applications of DFT are based on approximations

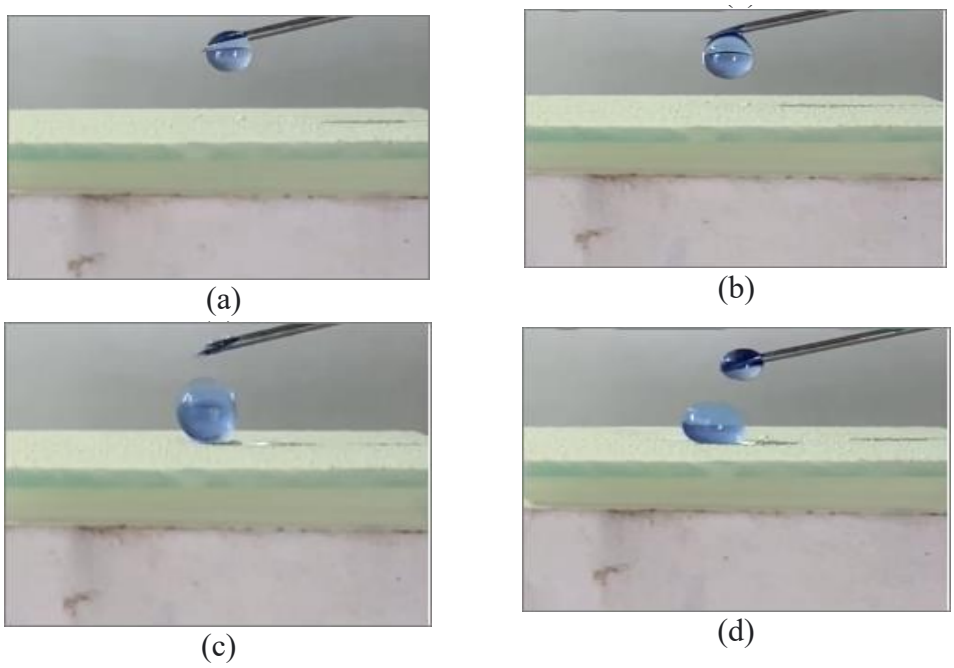

Fig. 2. The stages of a drop of water falling on the surface of the hydrophobic nanocomposite.

for the seeming exchange-correlation potential that gives superior accuracy to Hartree-Fock theory (Ab-initio and semiemperical approximations).

The exchange-correlation potential describes the influence of the Pauli principle and the Coulomb potential beyond a pure electrostatic interaction of the electrons. Possessing the perfect exchange-correlation potential means that: the many-body problem solved exactly [20].

MATERIALS AND METHODS

The study procedures included two parts, the first part is practical and the second part is simulation. In this work, films were prepared from polymeric composites [SiO_2 - TiO_2 / silane-cellulose acetate] on glass substrates using (0, 10:1, 10:2, 10:3, 10:4) of (SiO_2:TiO_2) weight ratio. Substrates were cleaned using absolute ethanol for 10 min and washing again with deionized water. The substrates dried with before the spraying process. Silane and cellulose acetate were added to the alcohol. SiO_2 and TiO_2 nano particle has been added with different weight percentages for the solution. To obtain a homogeneous mixture, the solution was mixed using a magnetic stirrer for 10 minutes, and then the solution was placed in an ultrasonic homogenizer for 15 minutes.The process of preparing the films was carried out using a thermal spray system on the glass bases at a temperature of 70 ° C.

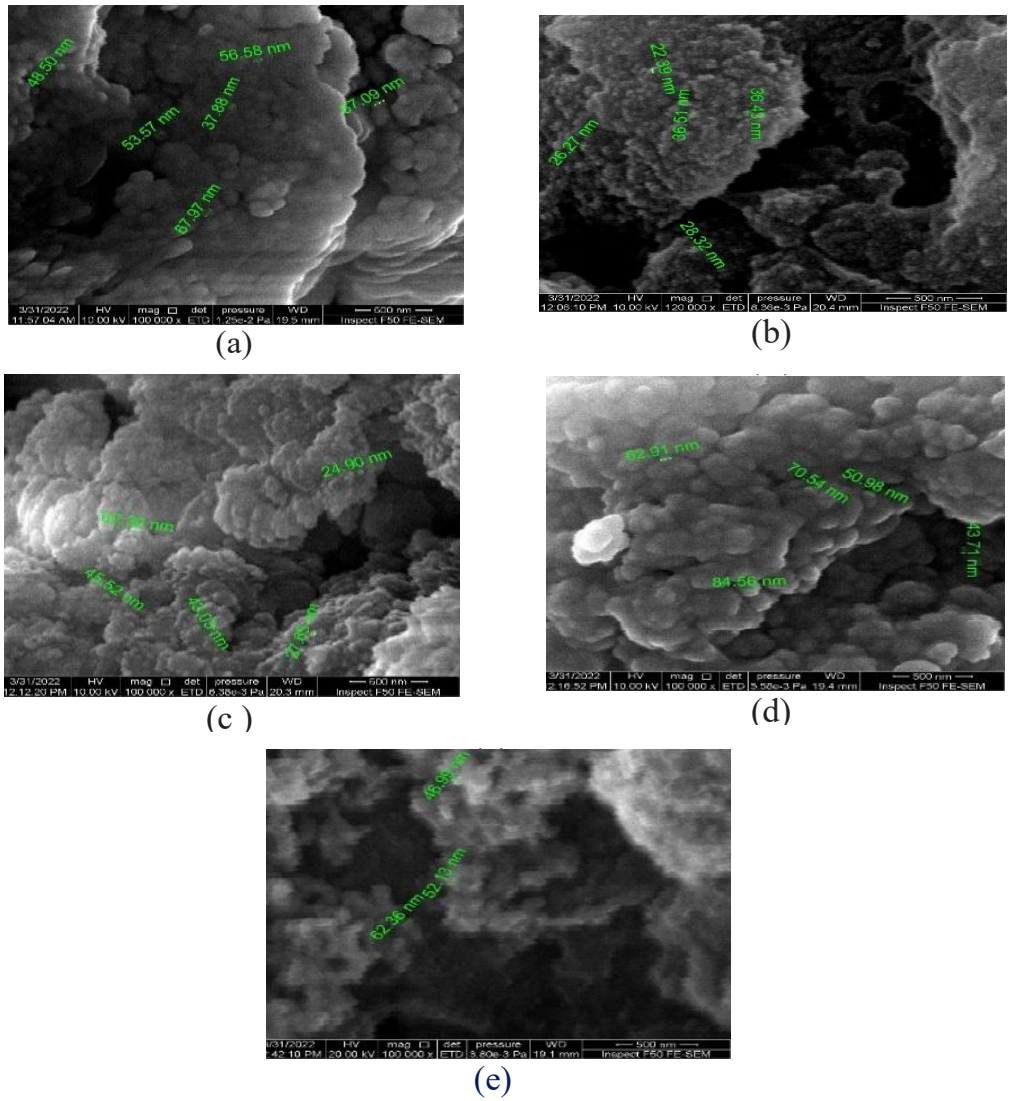

Fig. 3. FESEM images of films with (0, 10:1, 10:2, 10:3, 10:4) of (SiO_2:TiO_2) weight ratio.

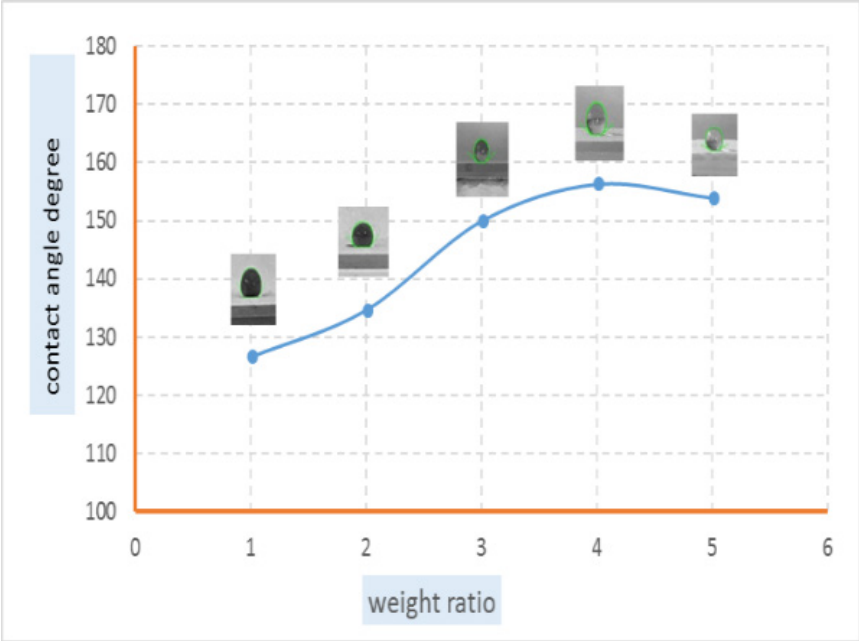

Fig. 4. The relation shape between TiO_2 weight ratio and WCA.

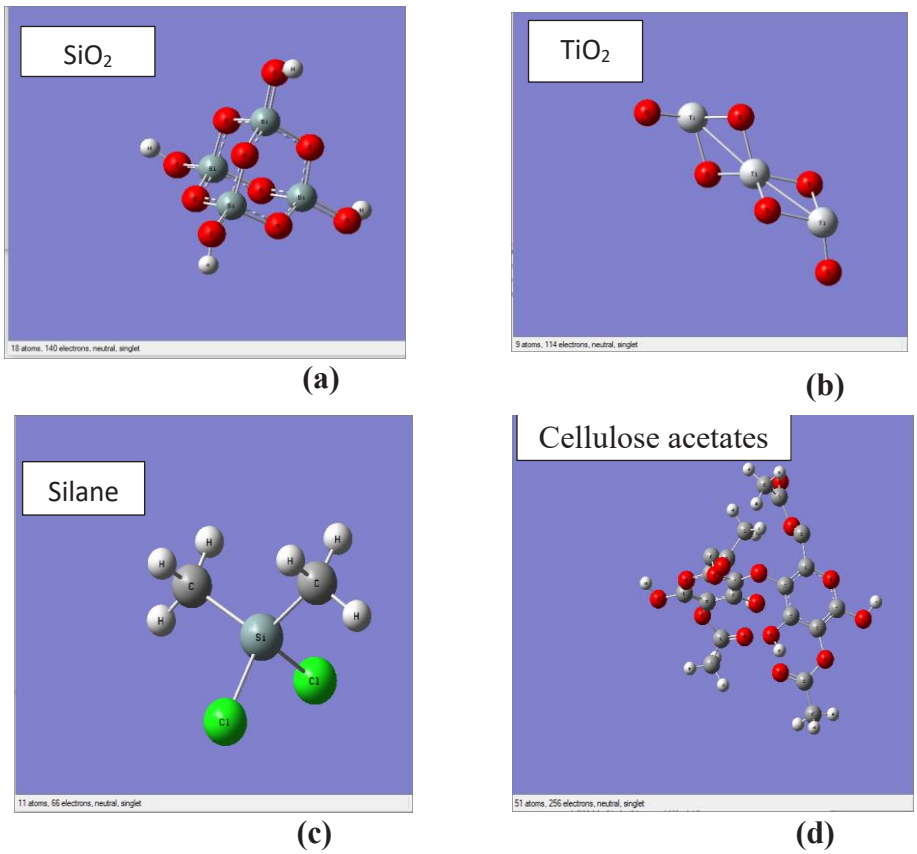

Fig. 5. the optimum stereo structure of silicon dioxide, titanium dioxide, silane and cellulose acetates.

Gauss view program has been designed to receive the input files from Gaussian program. Also, it is applied to display output files from Gaussian program with image dimensions. Gauss view does not use in calculations but it simplifies the work in Gaussian program and provides the users with three main benefits: The first, it makes the employer to draw the molecules; also, it enables to rotation, transformation and modification the size through the mouse. The second, it permits to investigate many Gaussian calculations, it deals with the complication in input setting for routine work by a progressive ways. The third, it allows to inspect of Gaussian calculations results by employ various geometrical techniques and this connect with equilibrium of molecular model, molecular orbital and electronic density surface [21].

RESULTS AND DISCUSSION

Hydrophobic nanocomposites were obtained through an overlapping mixture of nanomaterials (0, 10:1, 10:2, 10:3, 10:4) of (SiO_2:TiO_2) weight ratio with the matrix material (silan-cellulose acetate) using different weight ratios. Fig. 2 represents the stages of a drop of water falling on the surface of the nanocomposite. We note that the drop rolls off the surface and is not absorbed or adsorbed by the surface of the composite material, an indication of obtaining hydrophobic surface.

Microscopic images (FESEM) of the hydrophobic

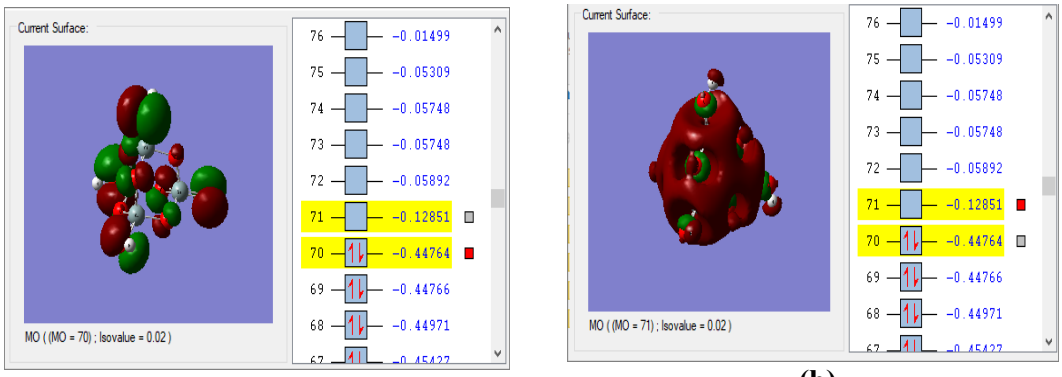

(a) (b)

Fig. 6. HOMO and LUMO of SiO_2.

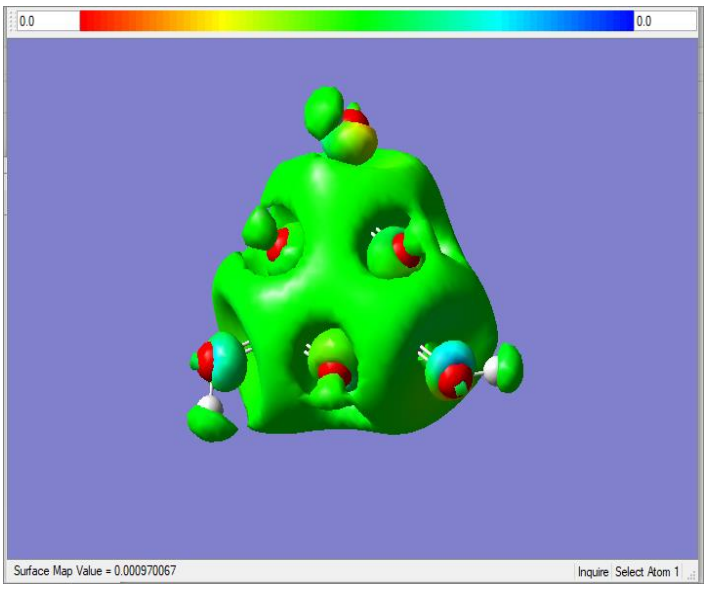

Fig. 7. Total potential energy of SiO_2.

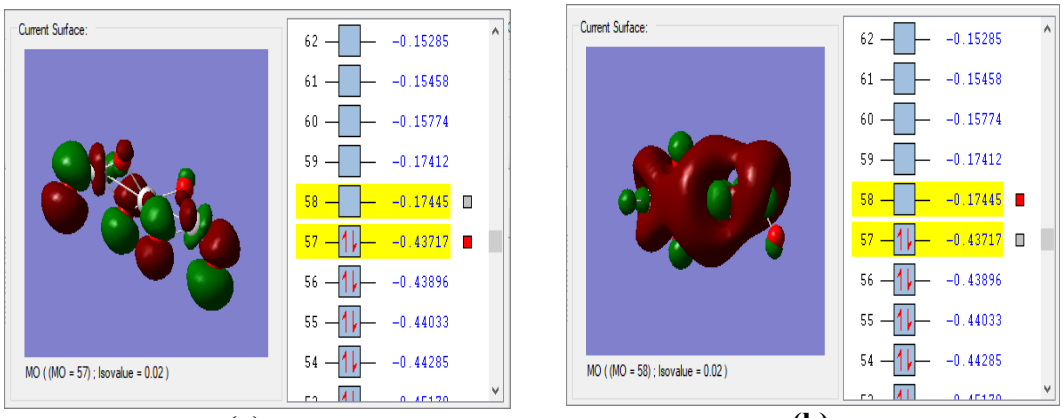

(a) **(b)**

Fig. 8. HOMO and LUMO of TiO_2.

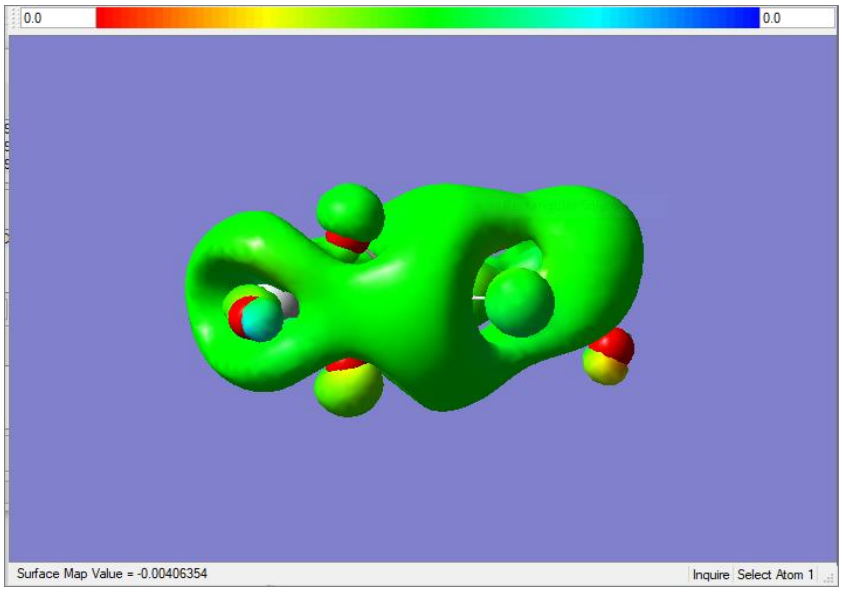

Fig. 9. Total potential energy of TiO_2.

film coated on glass substrate surfaces are shown in Fig. 3 and for all the weight ratios added to the matrix material. Fig. 3 reveals the FESEM images of manufactured films nanostructures of (0, 10:1, 10:2, 10:3, 10:4) of (SiO_2:TiO_2) weight ratio. Images shows presence of rock breakers nanostructures with rough and agglomeration with diameter range 23.39 nm to 84.56 nm.

Fig. 4 gives the relation shape between the effect of weight ratio and WCA of SiO_2 to TiO_2 nanostructures. The surface wettability measurements showed that the WCA increases from (126°) to (156 °). The optimum weight ratio is 10:3 with maximum CA equal 156.2 degree.

The simulation results included several properties. The first of these properties is to prove the optimization structure of each material that was used in the research. Fig. 5 shows the optimum stereo structure of silicon dioxide, titanium dioxide, silane and cellulose acetates. Fig. 5 shows the molecules structure and how the optimum structure was obtained, which benefits and helps to form an optimized composite material for the purpose of using it as a hydrophobic substance.

The density functional theory was used in this research by employing (6-31 g (d)) as a basis set and with the help of the wave function (B3LYP) to obtain the structural results related to the lengths of bonds, triangles, and dihedral angles.

The Figs. 6 and 8 represent the electronic distribution in the valence band, which is called HOMO, and the electronic distribution in the conduction band, called LUMO of SiO_2 and TiO_2 respectively. The red color represents the ionization potential, while the green color represents the electronic affinity of of SiO_2 and TiO_2 respectively.

Figs. 7 and 9 represents the total potential energy of SiO_2 and TiO_2, which is equal to zero. It can be noted that there is great stability represented by the green color, with a small presence of the ionization potential, which represents the red color.

CONCLUSION

The results showed that all films possess the property of self-clean surfaces. The addition of TiO_2 improved this property of hydrophobicity. The contact angles that content TiO_2 nanoparticles of the films were greater than that of the pure film. The optimal value of weight ratio was at the ratio 10: 3 with a contact angle equal to 156.2, so the films acquired the super hydrophobic surfaces.

The simulation gave a clear understanding of the optimal spatial structure of the molecules that build up the composite under study. It can be concluded that the simulation was able to analyze the surface property of the composite and the reason for it having a hydrophobic property.

CONFLICT OF INTEREST

The authors declare that there is no conflict of interests regarding the publication of this manuscript.

REFERENCE

1. Zhang P, Lv FY. A review of the recent advances in superhydrophobic surfaces and the emerging energy-related applications. Energy. 2015;82:1068-1087.
2. Si Y, Guo Z. Superhydrophobic nanocoatings: from materials to fabrications and to applications. Nanoscale. 2015;7(14):5922-5946.
3. Nosonovsky M, Bhushan B. Superhydrophobic surfaces and emerging applications: Non-adhesion, energy, green engineering. Current Opinion in Colloid & Interface Science. 2009;14(4):270-280.
4. Yao X, Song Y, Jiang L. Applications of Bio-Inspired Special Wettable Surfaces. Adv Mater. 2010;23(6):719-734.
5. Ma M, Hill RM. Superhydrophobic surfaces. Current Opinion in Colloid & Interface Science. 2006;11(4):193-202.
6. Richard E, Aruna ST, Basu BJ. Superhydrophobic surfaces fabricated by surface modification of alumina particles. Applied Surface Science. 2012;258(24):10199-10204.
7. Spraying Preparation of Eco-Friendly Superhydrophobic Coatings with Ultralow Water Adhesion for Effective Anticorrosion and Antipollution. American Chemical Society (ACS).
8. Feng J, Zhong L, Guo Z. Sprayed hieratical biomimetic superhydrophilic-superhydrophobic surface for efficient fog harvesting. Chem Eng J. 2020;388:124283.
9. Li Y, Chen S, Wu M, Sun J. All Spraying Processes for the Fabrication of Robust, Self-Healing, Superhydrophobic Coatings. Adv Mater. 2014;26(20):3344-3348.
10. Li J, Wu R, Jing Z, Yan L, Zha F, Lei Z. One-Step Spray-Coating Process for the Fabrication of Colorful Superhydrophobic Coatings with Excellent Corrosion Resistance. Langmuir. 2015;31(39):10702-10707.
11. Qian Z, Wang S, Ye X, Liu Z, Wu Z. Corrosion resistance and wetting properties of silica-based superhydrophobic coatings on AZ31B Mg alloy surfaces. Applied Surface Science. 2018;453:1-10.
12. Zhang X-F, Zhao J-P, Hu J-M. Abrasion-Resistant, Hot Water-Repellent and Self-Cleaning Superhydrophobic Surfaces Fabricated by Electrophoresis of Nanoparticles in Electrodeposited Sol-Gel Films. Advanced Materials Interfaces. 2017;4(13):1700177.
13. Lahiri SK, Zhang P, Zhang C, Liu L. Robust Fluorine-Free and Self-Healing Superhydrophobic Coatings by H_3BO_3 Incorporation with SiO_2–Alkyl-Silane@PDMS on Cotton Fabric. ACS Applied Materials & Interfaces. 2019;11(10):10262-10275.
14. Zhao W, Zhu R, Jiang J, Wang Z. Environmentally-friendly superhydrophobic surface based on Al_2O_3@KH560@SiO2 electrokinetic nanoparticle for long-term anti-corrosion in sea water. Applied Surface Science. 2019;484:307-316.
15. Kherrouba A, Bensegueni R, Guergouri M, Boulkedid A-L, Boutebdja M, Bencharif M. Synthesis, crystal structures, optical properties, DFT and TD-DFT studies of Ni (II) complexes with imine-based ligands. Journal of Molecular Structure. 2022;1247:131351.
16. Morjan IP, Dutu E, Fleaca CT, Dumitrache F, Morjan I, Mihailescu N, et al. Effect of annealing on the structural, optical and electrical properties of (F, Zn) double doped SnO_2 nanoparticles obtained by the laser pyrolysis method. Mater Sci Semicond Process. 2022;142:106511.
17. Heiba ZK, Mohamed MB, Farag NM, Badawi A. Structural, optical and electronic characteristics of Cu and Mg-doped nano MnS sample prepared by molten salt solid state reaction. Journal of Materials Science: Materials in Electronics. 2022;33(13):10388-10398.
18. Wen Q, Guo Z. Recent Advances in the Fabrication of Superhydrophobic Surfaces. Chem Lett. 2016;45(10):1134-1149.
19. Weser O, Freitag L, Guther K, Alavi A, Li Manni G. Chemical insights into the electronic structure of Fe(II) porphyrin using FCIQMC, DMRG, and generalized active spaces. American Chemical Society (ACS); 2020.
20. Culpitt T, Peters LDM, Tellgren EI, Helgaker T. Ab initio molecular dynamics with screened Lorentz forces. I. Calculation and atomic charge interpretation of Berry curvature. The Journal of Chemical Physics. 2021;155(2):024104.
21. Mohrdieck C. Physical Chemistry for the Life Sciences. By Peter Atkins and Julio de Paula. Chemphyschem. 2006;7(5):1149-1149.